Heliyon 9 (2023) e13009

Contents lists available at ScienceDirect

Heliyon

journal homepage: www.cell.com/heliyon

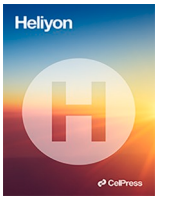

Research article

Spectrophotometric and nucleic acid-binding properties of halloysite clay nanotubes and kaolinite

Shubha R.L. Malla [a], Archana Gujjari [a], Carlos E. Corona [b], Gary W. Beall [a,b], L. Kevin Lewis [a,b,*]

[a] *Materials Science, Engineering and Commercialization Program, Texas State University, 601 University Drive, San Marcos, TX, 78666, USA*
[b] *Department of Chemistry and Biochemistry, Texas State University, 601 University Drive, San Marcos, TX, 78666, USA*

ARTICLE INFO

Keywords:
Nanotube
Nanoclay
Gene delivery
Drug delivery
Gene therapy
Nonviral vectors

ABSTRACT

Halloysite particles (HNTs) are naturally occurring aluminosilicate nanotubes of low toxicity that have shown great promise for drug and biomolecule delivery into human and animal cells. Kaolinite particles retain the same layered structure as HNT, but do not form nanotubes. In this study, the spectrophotometric and sedimentation properties of the two clays in aqueous solutions and their abilities to associate with both small and large nucleic acids have been investigated. Both clays scattered ultraviolet light strongly and this characteristic of HNT was not affected by either vacuum treatment to remove trapped gases or by sonication. Vacuum treatment increased the binding of small nucleic acids to HNT and this association was further enhanced by addition of divalent metal ions. By contrast, only small RNAs were bound efficiently by kaolinite in the presence of Mg^{2+} ions. Large linear double-stranded DNAs and circular plasmid DNAs bound poorly to kaolinite under all conditions, but these nucleic acids could form strong associations with HNT. Differences in binding data were largely consistent with measurements of the available surface areas of each clay. These results demonstrate that interactions with each clay are critically dependent on both the type and the conformation of each nucleic acid.

1. Introduction

Halloysite (HNT) is an aluminosilicate clay mineral that occurs naturally. The chemical formula of the clay is $Al_2Si_2O_5(OH)_4.nH_2O$ [1,2]. It is chemically similar to kaolinite but differs in having a hollow tubular structure and the presence of water in the interlayer spaces [3–6]. HNT nanotubes have a luminal diameter of approximately 15 nm and the outside diameter ranges from 50 to 70 nm. The lengths of HNT cylinders range between 500 and 2000 nm. The clay has a multilayered structure, with walls that are composed of 10–15 bilayers of octahedrally-coordinated aluminum and tetrahedrally-coordinated silicon atoms. The HNT tubes can be represented as rolled up scrolls of single layers of kaolinite [3,7].

Due to its layered structure, HNT has two types of surfaces. The inner face of the lumen that runs the length of the tube is covered with hydroxyl groups bonded to an alumina layer. They are also present between the layers of the scroll. When compared to kaolinite, the density of surface hydroxyl groups of HNTs is smaller [7–10]. The outer layer of each tube is a siloxane surface composed of a network of Si–*O*–Si bonds. The alumina groups located on the surface of HNT can help in formation of hydrogen bonds between HNT and biological components [9–15]. Due to different dielectric and ionization properties of silicon and aluminum oxides, the outer and

* Corresponding author. Chemistry and Biochemistry, Texas State University, 601 University Drive, San Marcos, TX, 78666, USA.
E-mail address: LL18@txstate.edu (L.K. Lewis).

https://doi.org/10.1016/j.heliyon.2023.e13009
Received 11 November 2022; Received in revised form 9 January 2023; Accepted 12 January 2023
Available online 16 January 2023

inner surfaces of HNT nanotubes are oppositely charged in water at pH values ranging from 3 to 8 [16].

Gene therapy has become an important option for treatment of human genetic disorders and cancer in recent years. This type of therapy involves several different approaches in practice, including use of CRISPR, siRNA and other methods requiring the transfer of nucleic acids directly into cells [17–20]. These approaches permit editing of genes within DNA and targeted modulation of gene expression. DNA and RNA are vulnerable to chemical and enzymatic degradation inside cells and cannot penetrate through cell membranes easily and therefore a protective carrier is often used [18,21,22]. Both viral and nonviral carriers have been employed for delivery and there is a necessity to develop improved vector systems for delivering nucleic acids into target cells and tissues without detrimental side effects.

Clay nanomaterials have shown great promise as protective gene carriers. HNTs are considered advantageous over other nanotubes, e.g., carbon nanotubes or inorganic nanotubes made of tungsten or titanium, etc. [21]. Due to the defined diameters of HNT nanotubes, only molecules with specific sizes can enter the lumen, providing regioselectivity [23–26]. Potential applications of HNT in drug delivery and nanobiomedicine are being actively studied [1,2,26,27]. HNT has been used as a natural vehicle for microencapsulation and controlled release of nucleic acids as well as both lipophilic and hydrophilic drugs [28–39]. In addition, clays such as HNT and kaolinite have the ability to adsorb/remove heavy metals and industrial chemicals [40–43].

The aim of this study was to analyze the association of small and large nucleic acids with halloysite and with the chemically similar but structurally different clay kaolinite. The binding affinities of different forms of single-stranded DNA (ssDNA), double-stranded DNA (dsDNA) and single-stranded RNA (ssRNA) were assessed and factors affecting adsorption efficiencies identified.

2. Materials and methods

2.1. Materials

Powdered halloysite, high molecular weight linear *E. coli* DNA (D2001) and metal chlorides were purchased from Millipore-Sigma. Kaolinite (KGa-1b) was obtained from The Clay Minerals Society (Purdue University). Halloysite nanotubes had lengths of 1–3 μm and diameters of 30–70 nm and previously reported cation exchange capacity of 8.0 meq/g. Kaolinite preparations contained 95–100% kaolin with 1–2% crystalline silica-quartz and cation exchange capacity of 0.02 meq/g (data from Clay Minerals Society). RNA and DNA oligonucleotides were purchased from Integrated DNA Technologies and ThermoFisher Scientific. The plasmid pRS316 has been described [44]. Agarose was obtained from Gold Biotechnology. Electrophoresis was performed using 11 × 14 cm Horizon gel rigs (Labrepco) as described [45]. Vacuum treatment of HNT solutions was performed for 5 min within an SC110 Speed Vac chamber containing an attached Savant GP110 pump.

2.2. UV–Vis spectroscopy

A Cary 100 Bio UV–Vis spectrophotometer or a BioRad SmartSpec 3000 spectrophotometer was used for spectroscopic absorbance measurements and scanning of HNT samples. A 3.5 mL quartz cuvette was used for UV spectra measurements. Three forms of HNT: untreated, vacuumed and sonicated, were prepared in deionized water (dH_2O) and scanned from 200 to 800 nm. Results of clay concentration-dependence tests were plotted as best fit trendlines using Microsoft Excel and default program parameters. Sonication was performed using a Vibracell VC501 Sonicator from Sonics & Materials for 5 min at an amplitude of 60 using a 3 mm probe tip. Assays were performed using four or five replicates and averages and standard deviations presented in the figures. All spectrophotometry-based experiments used 1.5 mL Eppendorf tubes previously shown to exhibit minimal leaching of light absorbing small molecules from the polypropylene plastic [46].

2.3. Preparation of nucleic acids

Double-stranded oligonucleotide DNA was prepared by mixing equimolar aliquots of Pvu4a and cPvu4a into a solution of 5 mM Tris (pH 7.5) to produce a final concentration of 300 ng/μL total DNA. The DNAs were denatured at 95 °C for 5 min and allowed to anneal while cooling to room temperature for 30 min. Complete annealing of the ssDNAs to form dsDNA was confirmed by gel electrophoresis using 3% agarose gels run in 0.5 × TB buffer. The gels were run at 200 V for 30 min and stained with ethidium bromide.

pRS316 plasmid DNA was extracted from *E. coli* DH5alpha cells using QIAprep miniprep kits from Qiagen. Purity and removal of RNA was confirmed by gel electrophoresis on 0.7% agarose gels run in 1 × TAE buffer. Quantitation was performed by measuring absorbance at 260 nm and calculating concentration based on the relationship that an A_{260} of 1.0 is equal to 50 μg/mL dsDNA. The quality of the linear chromosomal DNA employed in the assays was also confirmed using agarose gel electrophoresis.

2.4. Preparation of clay and nucleic acid solutions for adsorption assays

Clay-DNA and clay-RNA assays were typically performed by mixing 75 μL of clay (1, 2, 4 or 8 mg/mL), ~10 μL DNA or RNA (producing a final A_{260} of 1.0) and dH_2O in a final volume of 150 μL. Assay mixtures were shaken for 15 min at RT and centrifuged at 21,000 g for 30 min at 20 °C. The top 60 μL of supernatant was transferred into a new tube immediately after centrifugation and the A_{260} was measured. The percentage of DNA or RNA bound to HNT could be calculated by subtracting the absorbance of the supernatant (representing unbound nucleic acids that were not sedimented with the clay particles) from the original nucleic acid-only absorbance and dividing the resulting value by original nucleic acid-only absorbance. Averages and standard deviations resulting from tests of four

to five samples were determined.

2.5. Specific surface area analysis of HNT and kaolinite nanoparticles

Surface area tests were performed using a NOVAtouch LX2 gas sorption analyzer in conjunction with software from Quantachrome Instruments. Powdered HNT and kaolinite (0.1–0.2 g) were degassed by heating at 10 °C/min up to 200 °C and holding for 120 min. Physisorption volumes of ultra high purity nitrogen gas were then assessed. Six replicates were performed and results were averaged.

3. Results

3.1. Spectrophotometric and sedimentation properties of HNT

The goal of this study was to analyze the association of DNAs and RNAs consisting of different sizes and structures with HNT nanotubes and kaolinite nanoparticles. Kaolinite molecules have similar chemical and layered structures to those of HNT particles, but they are noncylindrical. In initial experiments, the optical and sedimentation properties of HNT were investigated. Light absorbance/scattering properties were assessed using three forms of the nanoclay. In addition to simple, well-mixed suspensions of the clay in water, both vacuumed and sonicated HNT solutions were analyzed using UV–Vis spectrophotometry. Vacuum treatment was performed to determine if removal of air trapped within the lumens of the nanotubes might influence their spectroscopic and/or nucleic acid binding properties. We note that exposure of HNT suspensions to a vacuum consistently resulted in temporary bubbling at their surfaces, a phenomenon that was not seen in control aqueous solutions; this result indicated that trapped air was present. Sonication was tested because it can break apart particles that have become noncovalently attached to each other. This treatment can increase the total surface area available for adsorption and therefore is potentially capable of influencing the binding efficiency of nucleic acids.

Spectroscopic scans of the three different types of HNT (untreated, vacuumed and sonicated) at 100 μg/mL in dH_2O were

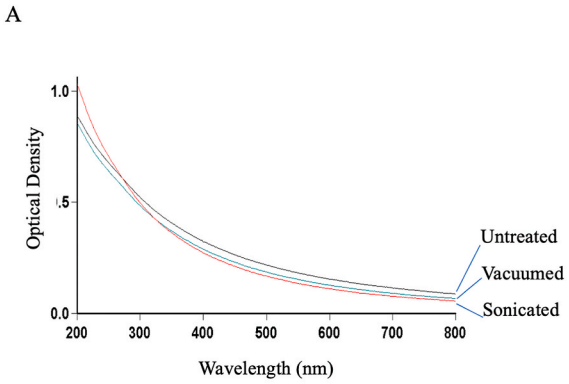

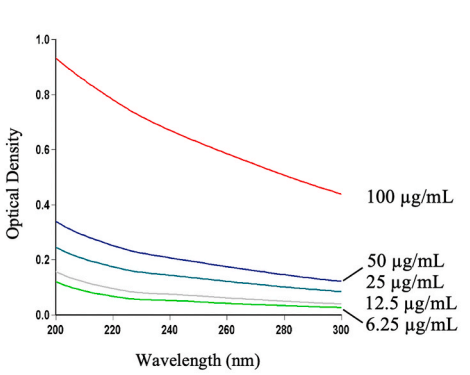

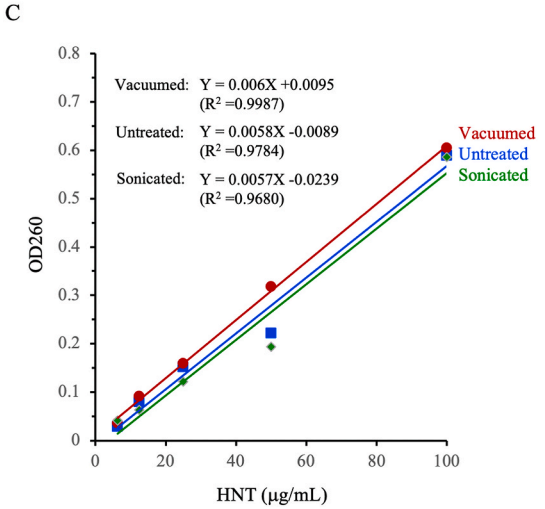

D

	Starting [HNT]	After centrifugation		
		OD260	[HNT]	HNT Remaining
Untreated HNT	1 mg/mL	0.0043	0.0023	0.2%
	0.5 mg/mL	0.0037	0.0022	0.4%
	0.25 mg/mL	0.0003	0.0016	0.6%
Vacuumed HNT	1 mg/mL	0.0177	0.0014	0.1%
	0.5 mg/mL	0.0057	0.0000	0.0%
	0.25 mg/mL	0.0087	-0.0001	0.0%
Sonicated HNT	1 mg/mL	0.0717	0.0168	1.7%
	0.5 mg/mL	0.0487	0.0127	2.5%
	0.25 mg/mL	0.0370	0.0107	2.3%

Fig. 1. Spectrophotometric and sedimentation properties of halloysite in aqueous solutions. (A) Light scattering caused by treated and untreated forms of HNT (100 mg/mL). (B) Scattering is concentration-dependent over a broad range of wavelengths. (C) Scattering at 260 nm is similar for treated and untreated HNT and linearly related to clay concentration. (D) Untreated and vacuumed HNT are sedimented more efficiently than sonicated HNT after centrifugation at 21,000 g for 30 min.

performed (Fig. 1A). The scans revealed no significant differences among the three clay preparations in this characteristic; each of the three forms exhibited strong apparent absorbances characteristic of light scattering effects that were highest at wavelengths corresponding to ultraviolet light (below 400 nm). When a series of HNT suspensions prepared at concentrations ranging from 6.25 to 100 μg/mL were scanned from 200 to 300 nm, a concentration-dependent effect was observed. Scans of untreated HNT particles are shown in Fig. 1B and similar results were seen with vacuumed and sonicated HNT. Analysis of the absorbances of the three types of HNT solutions at 260 nm, the peak wavelength typically used to monitor nucleic acid concentrations in aqueous solutions, revealed a linear relationship between OD260 and concentration (Fig. 1C). Beer's law equations and R^2 values calculated for each HNT solution are shown in the figure.

The interaction of nucleic acids with HNT was assessed next using centrifugation binding experiments. In these experiments HNT-nucleic acid complexes are pelleted by centrifugation and the fraction of unbound nucleic acids left in the supernatant is quantitated by measuring the absorbance at 260 nm [47,48]. To perform the experiments accurately, it was important to determine the efficiency of sedimentation of HNT nanoparticles and to maximize their precipitation so that unsedimented particles could not contribute to the apparent absorbance of the supernatant. HNT solutions (untreated, vacuumed and sonicated) at three different concentrations were centrifuged at 21,000 g for 5, 15, 30 and 60 min at 20 °C. After centrifugation, the supernatant was collected and the OD260 was measured and converted to an HNT concentration using the Beer's law equations derived in Fig. 1C. As an example of this analysis, Fig. 1D shows the amount of HNT precipitated from the different solutions after centrifugation for 30 min. Untreated and vacuumed HNT suspensions were sedimented with greater than 99% efficiency. By contrast, precipitation of sonicated HNT particles was not as efficient, achieving only 97–98% HNT removal under these conditions. We speculate that this is because sonication-induced breakage created a small number of particles with reduced sizes that did not sediment as efficiently as the larger particles.

3.2. Association of small DNAs and RNAs with HNT

The sequences and structures of the nucleic acids used in this study are presented in Fig. 2. The initial focus was on small DNAs and RNAs, but interactions with larger circular plasmid and linear chromosomal DNAs commonly used in molecular biology labs were also analyzed. To quantitate binding of the nucleic acids to the clay, mixtures were incubated at RT and then centrifuged to pellet the nanotube particles plus any nucleic acid molecules that had adsorbed onto them (depicted schematically in Fig. 3A). The absorbance of the supernatant at 260 nm (A_{260}) was measured and used to calculate the amount of bound nucleic acid. The approach described here has been employed in several previous studies of the interaction of clays with biomolecules [47,49–54].

In the first set of experiments, ssDNA 25mers (Pvu4a) dissolved in dH_2O (initial $A_{260} = 1.0$, equivalent to approximately 33 ng/μL) were mixed with increasing amounts of HNT in aqueous solutions (Fig. 3B). Vacuumed and non-vacuumed HNT particles, which were previously found to sediment most efficiently (Fig. 1D), were selected for the test. The average percentages of ssDNA bound and standard deviations recorded at each concentration of HNT are shown in the figure. Only a small proportion of the ssDNA was adsorbed under these conditions, corresponding to only 23% and 29% (unvacuumed and vacuumed) at the highest clay concentration. Binding to vacuumed HNT was consistently higher than to untreated HNT, though the improvement was modest.

The next set of experiments was performed with vacuumed HNT since this treatment produced the best results in the initial binding experiments. Three nucleic acids (dsDNA, ssDNA and ssRNA 25mers) were mixed with increasing concentrations of HNT and the bound nucleic acid was plotted against HNT concentration (Fig. 3C). Adsorption of all nucleic acids was inefficient at the HNT concentrations employed (0.5–4.0 mg/mL). Binding of ssRNA was strongest, becoming approximately two-fold higher than ssDNA and dsDNA at the highest clay concentration (45% vs 18% and 24%).

To test the impact of metal cations, assays were performed with and without addition of Na^+ and Mg^{2+} ions. The effect of the metals

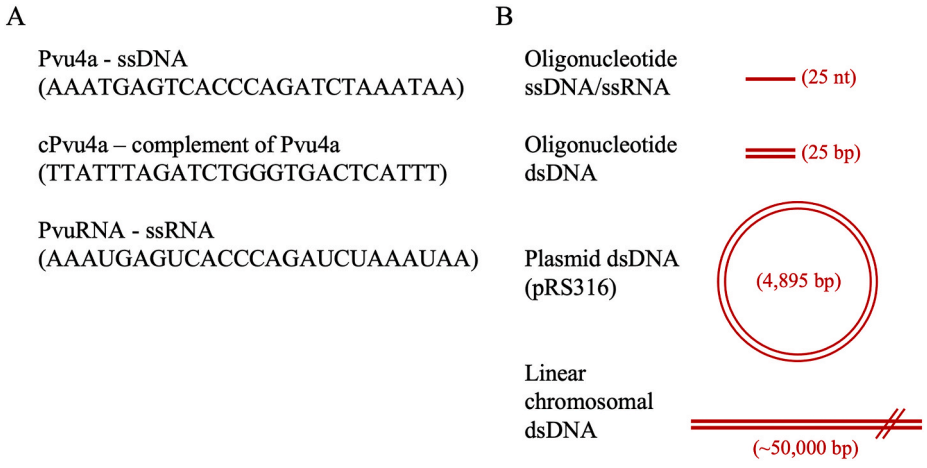

Fig. 2. Sequences and structures of nucleic acids used in the study. (A) Sequences of 25mer oligonucleotides. (B) Schematic representation of the sizes and structures of each nucleic acid.

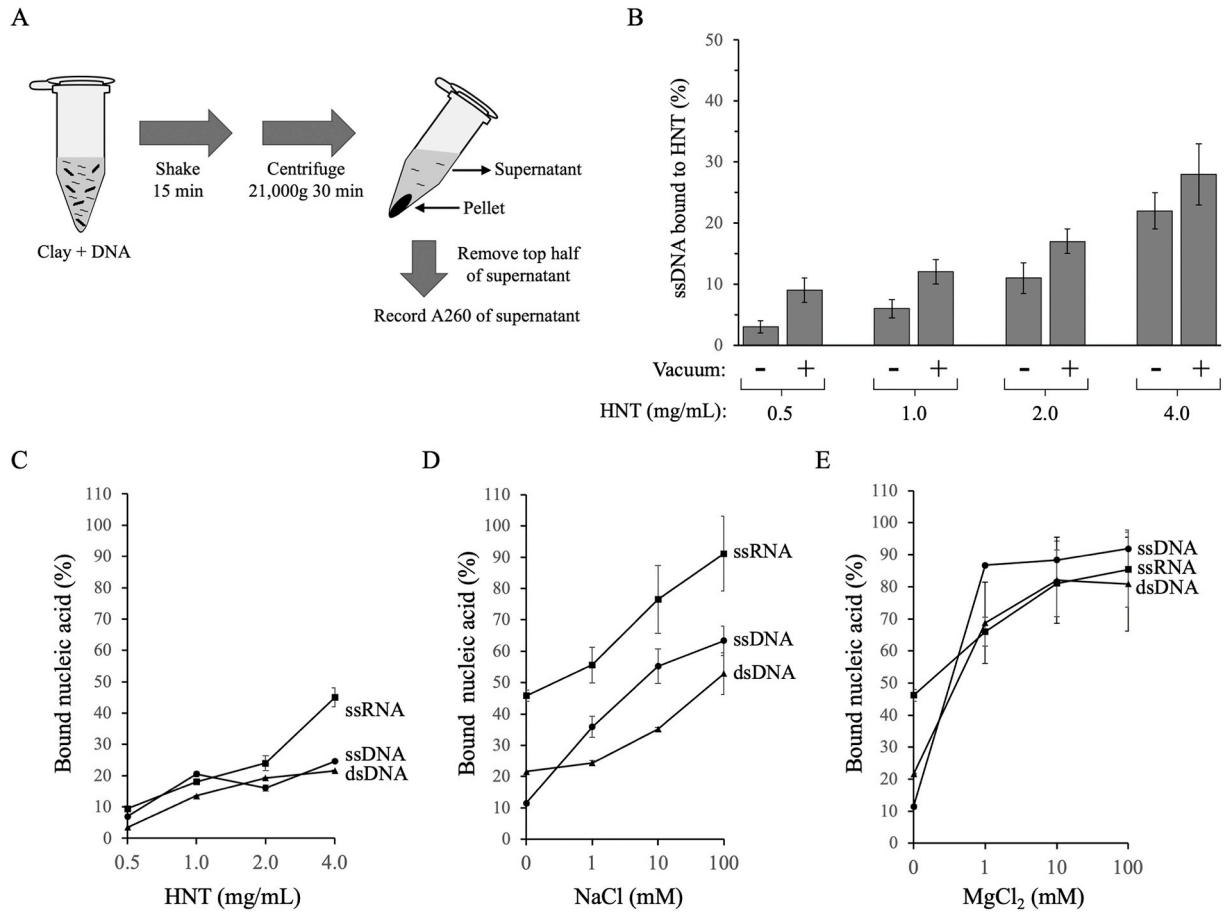

Fig. 3. Efficiencies of binding of small single-stranded and double-stranded nucleic acids to HNT. (A) Overview of binding assays. (B) Fraction of ssDNA (Pvu4a) adsorbed to untreated and vacuumed HNT particles. (C) Efficiency of binding of small nucleic acids to HNT without metals present. (D and E) Impact of sodium and magnesium ions on adsorption to 4 mg/mL HNT.

was assessed by adding 0, 1, 10, or 100 mM of each cation to the binding reactions (Fig. 3D and E). The fraction of bound nucleic acids increased at each concentration of Na^+ ions, reaching 91% for ssRNA, 63% for ssDNA, and 53% for dsDNA at 100 mM NaCl. Addition of magnesium ions produced strikingly different binding profiles from those seen with sodium (Fig. 3E). Adsorption increased strongly at 1 mM $MgCl_2$ and subsequently plateaued at 80–90% at the higher concentrations of 10 and 100 mM $MgCl_2$ for each of the nucleic acids.

3.3. Analysis of spectrophotometric and sedimentation characteristics of kaolinite

Kaolinite is a layered silicate clay that is chemically similar to HNT, but differs structurally. Spectrophotometric analysis of this clay suspended in aqueous solutions revealed that, like HNT, kaolinite exhibits concentration-dependent light scattering that is highest in the UV range of wavelengths (Fig. 4A). Sonication caused a modest increase in light scattering at 260 nm (Fig. 4B). This result suggests that a small fraction of the plate-like, multilayer complexes were joined to each other in the initial suspensions and could be broken apart by sonication. Centrifugation of 2 and 4 mg/mL kaolinite suspensions, performed as for HNT (Fig. 1D), showed that sedimentation was very efficient. Concentrations of both unsonicated and sonicated suspensions were reduced by more than 99.7% (Fig. 4C).

3.4. Binding of small DNAs and RNAs to kaolinite

Adsorption of small nucleic acids to kaolinite was extremely poor in the absence of metals. RNAs adsorbed the most efficiently, but maximum binding was only 12% (Fig. 5A), much less than that seen with HNT particles in Fig. 3C. Binding was improved by addition of sodium ions, especially at 10 and 100 mM NaCl. ssRNAs exhibited the highest adsorption at each metal concentration, reaching 47% at 100 mM NaCl (Fig. 5B). Magnesium ions strongly improved the binding of all nucleic acids at the lowest concentration (1 mM $MgCl_2$), increasing adsorption from $\leq$10% to approximately 50% (Fig. 5C). In contrast to the ssDNAs and dsDNAs, higher concentrations of the divalent metal ions stimulated a much larger increase in binding of ssRNAs to the kaolinite, reaching 87% bound at 100

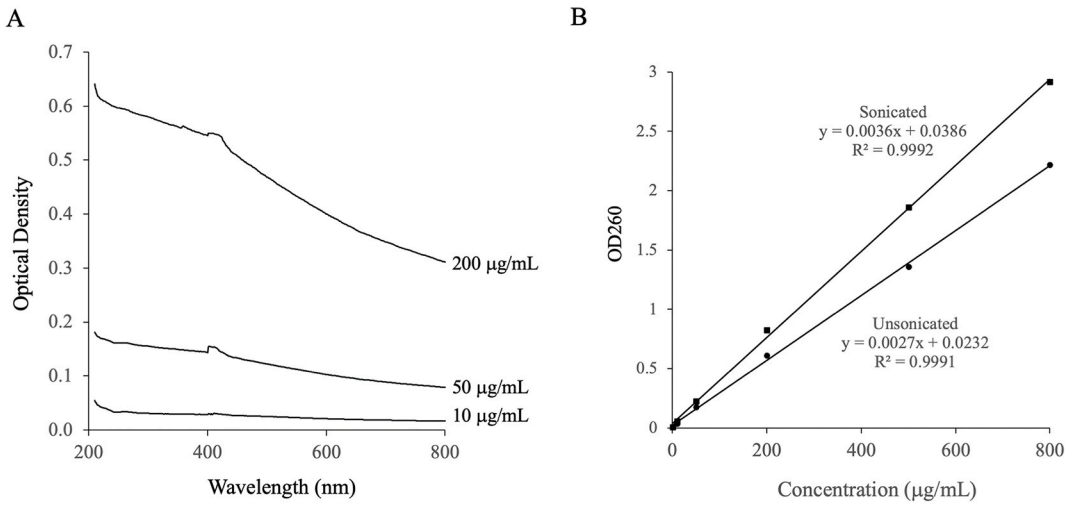

C

	Initial kaolinite concentration	After centrifugation: A260	After centrifugation: kaolinite remaining
Unsonicated	4 mg/mL	0.011	0.14%
	2 mg/mL	0.001	0.01%
Sonicated	4 mg/mL	0.030	0.28%
	2 mg/mL	0.008	0.15%

Fig. 4. Light scattering and sedimentation properties of kaolinite nanoparticles. (A) Light scattering is broadly concentration-dependent and greatest after exposure to ultraviolet light wavelengths. (B) Scattering at 260 nm by sonicated and unsonicated kaolinite suspensions. (C) Kaolinite is strongly sedimented by centrifugation at 21,000 g for 30 min.

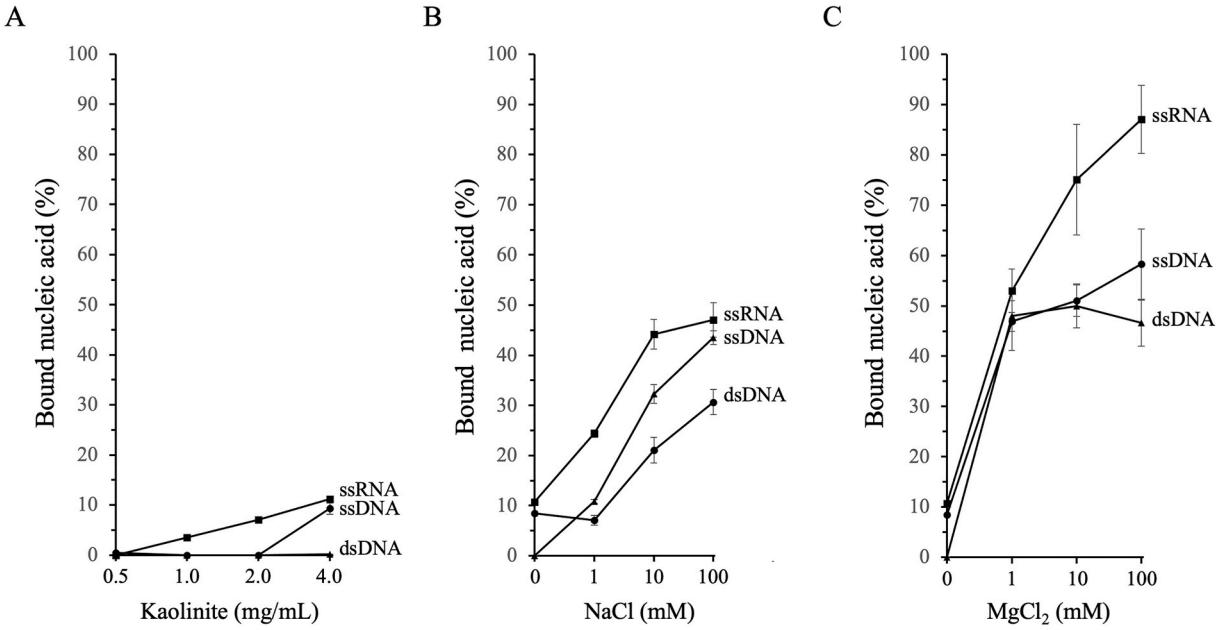

Fig. 5. Association of small nucleic acids with kaolinite nanoparticles. (A) Adsorption of single-stranded and double-stranded nucleic acids at different concentrations of clay. (B and C) Effect of addition of sodium and magnesium ions to binding reactions containing kaolinite (4 mg/mL).

mM $MgCl_2$.

3.5. Interaction of large circular and linear double-stranded DNAs with HNT and kaolinite

Binding of larger nucleic acids to HNT and kaolinite was evaluated using circular plasmid (pRS316, 4895 bp) and linear DNAs (*E. coli* chromosomal DNA fragments, ~50,000 bp). Adsorption of the plasmid DNA was similar to that of linear DNA at low concentrations of HNT, but became greater at higher clay concentrations, reaching 67% at 4 mg/mL clay vs. only 38% for the linear DNA (Fig. 6A). By contrast, binding of the nucleic acids to kaolinite without metals was much less efficient, reaching a maximum of only 22% (Fig. 6D). Interestingly, at 0.5 mg/mL HNT, binding of the circular DNAs was stimulated much more strongly in the presence of magnesium ions. The difference between circular and linear molecules was particularly apparent at 1 mM and 10 mM $MgCl_2$ (Fig. 6B). Addition of magnesium ions had only a modest effect on binding to kaolinite, with maximum adsorption reaching only 30% (Fig. 6E).

In a previous study of sedimentation of DNAs by addition of metal ions at high pH, we observed that calcium ions produced greater effects than magnesium ions [55]. To compare the impact of each metal on association with clays, the experiments shown in Fig. 6B and E were repeated using $CaCl_2$. Addition of 1, 10 and 100 mM calcium ions consistently resulted in higher levels of adsorption of circular DNAs than that seen with magnesium (compare Fig. 6B vs Fig. 6C). However, binding of linear DNAs was similar with the two metal cations. In contrast to the results observed with HNT, binding of the DNAs to kaolinite was similarly low when either magnesium or calcium was added (Fig. 6F).

3.6. Surface area analysis of the two clays

The large difference in DNA binding by HNT versus kaolinite was investigated further by assessing available surface areas on each clay. Nitrogen gas physiosorption tests of the dried, degassed clay powders revealed striking differences (Table 1). In two independent trials, surface area measurements for HNT were 38.6 and 39.9 m^2/g, but gas sorption to the kaolinite particles was undetectable.

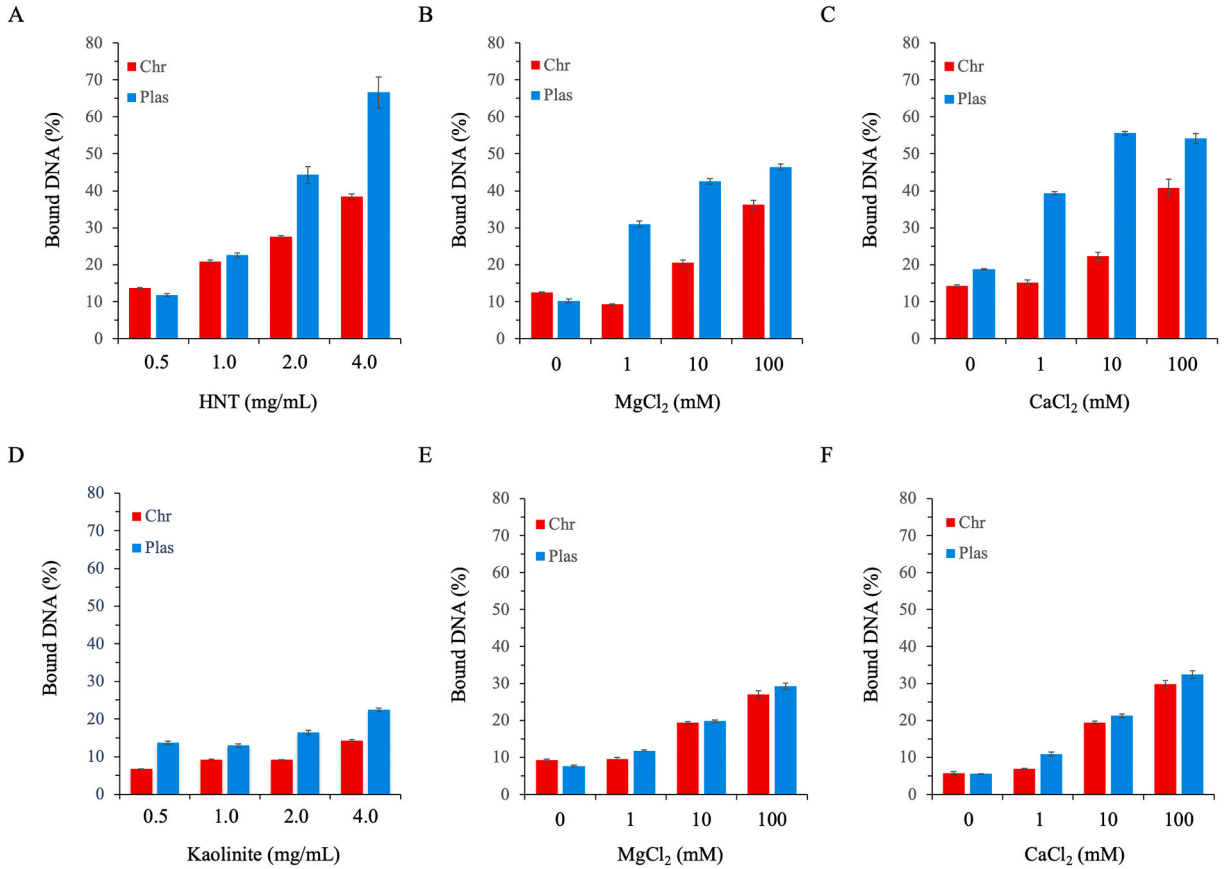

Fig. 6. Interaction of large linear chromosomal and circular plasmid DNAs with HNT and kaolinite. (A) Adsorption of DNAs to HNT without metals. (B and C) Binding of DNAs to 0.5 mg/mL HNT in the presence of magnesium or calcium ions. (D) DNA adsorption to kaolinite in the absence of metals. (E and F) Binding of large DNAs to 0.5 mg/mL kaolinite in the presence of magnesium or calcium ions.

Table 1

	Gas sorption (m^2/g)	
	HNT	Kaolinite
Trial 1	38.6 ± 0.4	0.0
Trial 2	39.9 ± 0.5	0.0

4. Discussion

In the current study we have analyzed the interactions of several nucleic acids comprised of different sizes and structures with halloysite and with the chemically similar but structurally different nanoclay kaolinite. Spectrophotometric scanning of aqueous HNT solutions revealed little change in their UV light scattering/absorbance properties when mixtures were either vacuumed to remove trapped air or sonicated to break up weakly attached particles. Similarly, sonication of the nontubular kaolinite particle suspensions also had only a modest impact on interactions with UV and visible light. Beer's law relationships could be established between apparent UV absorbances and the concentrations of the treated and untreated clays. These equations permitted monitoring of clay concentrations and determination of centrifugation parameters capable of sedimenting approximately 100% of the particles.

Centrifugation binding assays revealed that HNT has very low affinity for each of the three small nucleic acids when tested using simple aqueous solutions. Addition of Na^+ ions greatly increased the binding of RNAs to HNT, but had only a moderate effect on binding of the small single-stranded or double-stranded DNAs. By contrast, addition of Mg^{2+} ions strongly promoted the adsorption of all small nucleic acids to HNT, especially at low concentrations of the metal (1–10 mM). Overall, these results indicate that DNAs and RNAs have weak affinity for HNT, but the addition of metals, in particular Mg^{2+} at 1 mM or higher, strongly improves adsorption to HNT.

Binding of small nucleic acids to kaolinite in the absence of metal ions was consistently less efficient than to HNT. The ssRNAs were bound most strongly to the noncylindrical clay, with and without addition of metal ions. Although the presence of Mg^{2+} ions greatly increased binding of DNAs and RNAs to HNT (up to 80–90% adsorption), the divalent ions strongly increased association of only the ssRNAs with kaolinite (compare Fig. 3E vs Fig. 5C). It is likely that this increased binding of single-stranded species is due to the increased conformational flexibility and access to base groups compared to double-stranded nucleic acids. In addition, the oxygen at the 2′ position of ribose in the RNAs provides an additional contact for binding that is not available in the DNAs [56–58].

Interactions of large circular and linear dsDNA molecules (≥5000 bp in length vs only 25 for the small nucleic acids) identified unique characteristics of each of the clays. Binding of the large nucleic acids to HNT was more efficient than binding of oligonucleotides in the absence of metal ions. This was especially true for the circular plasmid DNAs, which exhibited strong adsorption at 2 and 4 mg/mL HNT. Binding of both types of large DNAs could be increased by addition of divalent metal ions, with the circular DNAs consistently showing the strongest affinities. Association of the larger nucleic acids with kaolinite was strikingly less efficient than that seen with HNT. For example, only 13% and 22% of linear and circular DNAs became bound to kaolinite particles at 4 mg/mL clay, while the corresponding numbers for HNT were 37% and 65%. Although addition of Mg^{2+} and Ca^{2+} ions increased adsorption of the larger DNAs to kaolinite, the effects were much less pronounced than with HNT. A previous study by Gupta et al. demonstrated that metals bind relatively poorly to kaolinite [59], which may explain, in part, the weaker impact of Mg^{2+} and Ca^{2+} ions on binding to this clay. In addition, the results of the gas sorption analysis presented here and some past studies of the clay point to a more general reduced surface area adsorption capability among kaolinite nanoparticles (Table 1) [40,60–63]. Interestingly, the limited natural adsorption capacity of kaolinite has been improved by synthetic conversion into cylinders and microspheres, structures with interior spaces analogous to HNT [64,65].

Removal of air from the lumens of HNT nanotubes improved DNA adsorption. This result provides an indication that binding was occurring in the lumen, though it does not exclude the possibility that some binding also occurred on the outer surface. The smallest diameters of the single-stranded and double-stranded nucleic acids used here are 1 and 2 nm, respectively, which is considerably smaller than the ~15 nm diameter of the lumens of the HNT nanotubes, suggesting that this space should be accessible. In addition, the Al_2O_3 inner surface of the lumen is slightly positively charged while the outer SiO_2 surface is negatively charged at neutral pH [66]. Thus, negatively charged DNAs and RNAs are likely to have a natural affinity for the interior surfaces of HNT.

We observed that binding to HNT was most strongly stimulated by addition of Mg^{2+} ions. This result is in accord with several past studies demonstrating that divalent cations such as Mg^{2+} and Ca^{2+} ions can promote strong associations between nucleic acids and clays [47–49,52–54,68,69]. Previous reports have suggested the possibility that small biomolecules may bind within the interior of HNT nanotubes and that some binding may also occur on the cylindrical outer perimeters [3–5,66,67]. The strong impact of the positively charged magnesium ions suggests that the negatively charged nucleic acids may be capable of adsorbing to the outer surface via ionic crosslinking (cation bridging) with the divalent metals, as seen with other clays [47,52,55,68,69]. It is likely that the improved binding in the presence of divalent ions involves several factors, resulting from increased charge density and charge shielding, the ability to participate in ionic crosslinking interactions, and the potential for direct binding to the phosphate, base and ribose moieties of the nucleic acids.

Author contribution statement

Shubha R. L. Malla, Ph.D.: Performed the experiments; Analyzed and interpreted the data.

Archana Gujjari, Ph.D., Carlos E. Corona, B.S: Performed the experiments.

Gary W. Beall, Ph.D.: Conceived and designed the experiments; Analyzed and interpreted the data.

L. Kevin Lewis, Ph.D.: Conceived and designed the experiments; Analyzed and interpreted the data; Contributed reagents, materials, analysis tools or data; Wrote the paper.

Funding statement

Professor L. Kevin Lewis was supported by National Institutes of Health [1R15GM139093-01].

Carlos E. Corona was supported by National Science Foundation Research Experiences for Undergraduates (REU) [1757843].

Data availability statement

Data will be made available on request.

Declaration of interest's statement

The authors declare that they have no known competing financial interests or personal relationships that could have appeared to influence the work reported in this paper.

Acknowledgments

The authors wish to thank Harish Kallagunta for use of gas sorption analysis facilities within his laboratories.

References

[1] M. Du, B. Guo, D. Jia, Newly emerging applications of halloysite nanotubes: a review, Polym. Int. 59 (2010) 574–582.
[2] E. Joussein, S. Petit, J. Churchman, B. Theng, D. Righi, B. Delvaux, Halloysite clay minerals-review, Clay Miner. 40 (2005) 383–426.
[3] E. Abdullayev, Y. Lvov, Halloysite clay nanotubes as a ceramic "skeleton" for functional biopolymer composites with sustained drug release, J. Mater. Chem. B 1 (2013) 2894–2903.
[4] S.R. Levis, P.B. Deasy, Characterization of halloysite for use as a microtubular drug delivery system, Int. J. Pharm. 243 (2002) 125–134.
[5] R. Kamble, M. Ghag, S. Gaikawad, B. Panda, Halloysite nanotubes and applications: a review, J. Adv. Sci. Res. 3 (2012) 25–29.
[6] Y. Lvov, W. Wang, L. Zhang, R. Fakhrullin, Halloysite clay nanotubes for loading and sustained release of functional compounds, Adv. Mater. 28 (2016) 1227–1250.
[7] T.F. Bates, F.A. Hildebrand, A. Swineford, Morphology and structure of endellite and halloysite, Am. Mineral. 35 (1950) 463–484.
[8] K.S. Birrell, M.W. Fieldes, K.I. Uiamson, Unusual forms of halloysite, Am. Mineral. 40 (1955) 122–124.
[9] D. Rawtani, Y.K. Agrawal, Multifarious applications of halloysite nanotubes: a review, Rev. Adv. Mater. Sci. 30 (2012) 282–295.
[10] M. Dor, Y. Levi-Kalisman, R.J. Day-Stirrat, Y. Mishael, S. Emmanuel, Assembly of clay mineral platelets, tactoids, and aggregates: effect of mineral structure and solution salinity, J. Colloid Interface Sci. 566 (2020) 163–170.
[11] J.H. Kirkman, Clay mineralogy of some tephra beds of Rotorua area, North Island, New Zealand, Clay Miner. 10 (1975) 437–449.
[12] J.H. Kirkman, Possible structure of halloysite disks and cylinders observed in some New Zealand rhyolitic tephras, Clay Miner. 12 (1977) 199–216.
[13] X. Wang, M.L. Weiner, Hydrogen Storage Apparatus Comprised of Halloysite, 2005. US Patent Specification: 0233199.
[14] R. Klimkiewicz, B.D. Edwarda, Catalytic activity of carbonaceous deposits in zeolite from halloysite in alcohol conversions, J. Phys. Chem. Solid. 65 (2004) 459–464.
[15] P. Pasbakhsh, H. Ismail, M.N.A. Fauzi, A. Abu Bakar, EPDM/modified halloysite nanocomposites, Appl. Clay Sci. 48 (2010) 405–413.
[16] L. Guimaraes, A.N. Enyashin, G. Seifert, H.A. Duarte, Structural, electronic, and mechanical properties of single-walled halloysite nanotube models, J. Phys. Chem. C 114 (2010) 11358–11363.
[17] C.E. Dunbar, K.A. High, J.K. Joung, D.B. Kohn, K. Ozawa, M. Sadelain, Gene therapy comes of age, Science 359 (2018) 6372.
[18] L. Duan, K. Ouyang, X. Xu, L. Xu, C. Wen, X. Zhou, Z. Qin, Z. Xu, W. Sun, Y. Liang, Nanoparticle delivery of CRISPR/Cas9 for genome editing, Front. Genet. 12 (2021), 673286.
[19] J.H. Goell, I.B. Hilton, CRISPR/Cas-based epigenome editing: advances, applications, and clinical utility, Trends Biotechnol. 39 (2021) 678–691.
[20] H. Adachi, M. Hengesbach, Y.T. Yu, P. Morais, From antisense RNA to RNA modification: therapeutic potential of RNA-based technologies, Biomedicines 9 (2021) 550.
[21] N.G. Veerabadran, R.R. Price, Y.M. Lvov, Clay nanotubes for encapsulation and sustained release of drugs, Nano 2 (2007) 115–120.
[22] R.K. DeLong, U. Akhtar, M. Sallee, B. Parker, S. Barber, J. Zhang, M. Craig, R. Garrad, A. Hickey, E. Engstrom, Characterization and performance of nucleic acid nanoparticles combined with protamine and gold, Biomaterials 30 (2009) 6451–6459.
[23] P. Pasbakhsh, H. Ismail, M.N.A. Fauzi, A. Abu Bakar, Influence of maleic anhydride grafted ethylene propylene diene monomer (MAH-g-EPDM) on the properties of EPDM nanocomposites reinforced by halloysite nanotubes, Polym. Test. 28 (2009) 548–559.
[24] H. Ismail, P. Pasbakhsh, M.N.A. Fauzi, A. Abu Bakar, Morphological, thermal and tensile properties of halloysite nanotubes filled ethylene propylene diene monomer (EPDM) nanocomposites, Polym. Test. 27 (2008) 841–850.
[25] H. Ismail, P. Pasbakhsh, M.N.A.A. Fauzi, Abu Bakar, the effect of halloysite nanotubes as a novel nanofiller on curing behaviour, mechanical and microstructural properties of ethylene propylene diene monomer (EPDM) nanocomposites, Polym.-Plast. Technol. Eng. (2009) 33–37.
[26] B. Guo, F. Chen, Y. Lei, X. Liu, J. Wan, D. Jia, Styrene-butadiene rubber/halloysite nanotubes nanocomposites modified by sorbic acid, Appl. Surf. Sci. 255 (2009) 7329–7336.
[27] K. Krejcova, P.B. Deasy, M. Rabishkova, Optimization of diclofenac sodium profile from halloysite nanotubes, Ces. Slov. Farm. 62 (2013) 71–77.
[28] S.R. Levis, P.B. Deasy, Use of coated microtubular halloysite for the sustained release of diltiazem hydrochloride and propranolol hydrochloride, Intl. J. Pharm. 253 (2003) 145–157.
[29] J. Forsgren, E. Jamstorp, S. Bredenberg, H. Engqvist, M. Stromme, A ceramic drug delivery vehicle for oral administration of highly potent opioids, J. Pharmacol. Sci. 99 (2010) 219–226.
[30] Y.F. Shi, Z. Tian, Y. Zhang, H.B. Shen, N.Q. Jia, Functionalized halloysite nanotube-based carrier for intracellular delivery of antisense oligonucleotides, Nanoscale Res. Lett. 6 (2011) 608.
[31] R.R. Price, Y.M. Lvov, In-vitro release characteristics of tetracycline HCl, khellin and nicotinamide adenine dinucleotide from halloysite; a cylindrical mineral, J. Microencapsul. 18 (2001) 713.

[32] Y. Lvov, R.R. Price, B. Gaber, I. Ichinose, Thin film nanofabrication via layer-by-layer adsorption of tubule halloysite, spherical silica, proteins and polycations, Colloids Surf. A Physicochem. Eng. Aspects 198–200 (2002) 375–382.
[33] V. Vergaro, Y.M. Lvov, S. Leporatti, Halloysite clay nanotubes for resveratrol delivery to cancer cells, Macromol. Biosci. 12 (2012) 1265–1271.
[34] M.T. Viseras, C. Aguzzi, P. Cerezo, C. Viseras, C. Valenzuela, Equilibrium and kinetics of 5-aminosalicylic acid adsorption by halloysite, Microporous Mesoporous Mater. 108 (2008) 112–116.
[35] S. Maisanaba, S. Pichardo, M. Puerto, D. Gutierrezooo-Praena, A.M. Camean, A. Jos, Toxicological evaluation of clay minerals and derived nanocomposites: a review, Environ. Res. 138 (2015) 233–254.
[36] Y.J. Suh, D.S. Kil, K.S. Chung, E. Abdullayev, Y.M. Lvov, D. Mongayt, Natural nanocontainer for the controlled delivery of glycerol as a moisturizing agent, J. Nanosci. Nanotechnol. 11 (2011) 661–665.
[37] N. Verma, E. Moore, W. Blau, Y. Volkov, P. Ramesh Babu, Cytotoxicity evaluation of nanoclays in human epithelial cell line A549 using high content screening and real-time impedance analysis, J. Nanopart. Res. 14 (2012) 1–11.
[38] L. Sun, D.K. Mills, Halloysite Nanotube-Based Drug Delivery System for Treating Osteosarcoma, in: 36th Ann. Intl. Conf. IEEE Engineering in Medicine and Biology Society, 2014, pp. 2920–2923.
[39] N. Khatoon, M.Q. Chu, C.H. Zhou, Nanoclay-based drug delivery systems and their therapeutic potentials, J. Mater. Chem. B. 8 (2020) 7335–7351.
[40] A. Septian, S. Oh, W.S. Shin, Sorption of antibiotics onto montmorillonite and kaolinite: competition modelling, Environ. Technol. 40 (2019) 2940–2953.
[41] V.B. Yadav, R. Gadi, S. Kalra, Clay based nanocomposites for removal of heavy metals from water: a review, J. Environ. Manag. 232 (2019) 803–817.
[42] M.R. Abukhadra, M. Mostafa, A.M. El-Sherbeeny, M.A. El-Meligy, A. Nadeem, Instantaneous adsorption of synthetic dyes from an aqueous environment using kaolinite nanotubes: equilibrium and thermodynamic studies, ACS Omega 6 (2020) 845–856.
[43] G. Cavallaro, G. Lazzara, E. Rozhina, S. Konnova, M. Kryuchkova, N. Khaertdinov, R. Fakhrullin, Organic-nanoclay composite materials as removal agents for environmental decontamination, RSC Adv. 9 (2019) 40553–40564.
[44] T.W. Christianson, R.S. Sikorski, M. Dante, S.H. Shero, P. Hieter, Multifunctional yeast high-copy-number shuttle vectors, Gene 110 (1992) 119–122.
[45] B.A. Sanderson, N. Araki, J.L. Lilley, G. Guerrero, L.K. Lewis, Modification of gel architecture and TBE/TAE buffer composition to minimize heating during agarose gel electrophoresis, Anal. Biochem. 454 (2014) 44–52.
[46] L.K. Lewis, M.H. Robson, Y. Vecherkina, C. Ji, G.W. Beall, Interference with spectrophotometric analysis of nucleic acids and proteins by leaching of chemicals from plastic tubes, Biotechniques 48 (2010) 297–302.
[47] G.W. Beall, D.S. Sowersby, R.D. Roberts, M.H. Robson, L.K. Lewis, Analysis of oligonucleotide DNA binding and sedimentation properties of montmorillonite clay using ultraviolet light spectroscopy, Biomacromolecules 10 (2009) 105–112.
[48] B.A. Sanderson, D.S. Sowersby, S. Crosby, M. Goss, L.K. Lewis, G.W. Beall, Charge density and particle size effects on oligonucleotide and plasmid DNA binding to nanosized hydrotalcite, Biointerphases 8 (2013) 8.
[49] E. Paget, L.J. Monrozier, P. Simonet, Adsorption of DNA on clay minerals: protection against, 1992 against DNase I and influence on gene transfer, FEMS Microbiol. Lett. 97 (1992) 31–40.
[50] M. Khanna, G. Stotzky, Transformation of Bacillus subtilis by DNA bound on montmorillonite and effect of DNase on the transforming ability of bound DNA Appl, Environ. Microbiol. 58 (1992) 1930–1939.
[51] F. Poly, C. Chenu, P. Simonet, J. Rouiller, L.J. Monrozier, Differences between linear chromosomal and supercoiled plasmid DNA in their mechanisms and extent of adsorption on clay minerals, Langmuir 16 (2000) 1233–1238.
[52] M. Franchi, J.P. Ferris, E. Gallori, Cations as mediators of the adsorption of nucleic acids on clay surfaces in prebiotic environments, Orig. Life Evol. Biosph. 33 (2003) 1–16.
[53] P. Cai, Q. Huang, X. Zhang, Microcalorimetric studies of the effects of MgCl2 concentrations and pH on the adsorption of DNA on montmorillonite, kaolinite and goethite, Appl. Clay Sci. 32 (2006) 147–152.
[54] B.V. Rodriguez, J. Pescador, N. Pollok, G.W. Beall, C. Maeder, L.K. Lewis, Impact of size, secondary structure, and counterions on the binding of small ribonucleic acids to layered double hydroxide nanoparticles, Biointerphases 10 (2015), 041007.
[55] C.J. England, T.C. Gray, S.R.L. Malla, S.A. Oliveira, B.R. Martin, G.W. Beall, L.K. Lewis, pH-dependent sedimentation of DNA in the presence of divalent, but not monovalent, metal ions, Anal. Biochem. 616 (2021), 114099.
[56] E. Freisinger, R.K.O. Sigel, From nucleotides to ribozymes-A comparison of their metal ion binding properties, Coord. Chem. Rev. 251 (2007) 1834–1851.
[57] J. Anastassopoulou, Metal-DNA interactions, J. Mol. Struct. 651–653 (2003) 19–26.
[58] M.H. Shamsi, H.-B. Kraatz, Interactions of metal ions with DNA and some applications, J. Inorg. Organomet. Polym. Mater. 23 (2013) 4–23.
[59] S. Sen Gupta, K.G. Bhattacharyya, Adsorption of heavy metals on kaolinite and montmorillonite: a review, Phys. Chem. Chem. Phys. 14 (2012) 6698–6723.
[60] J. Matusik, E. Wisla-Walsh, A. Gawel, E. Bielanska, K. Bahranowski, Surface area and porosity of nanotubes obtained from kaolin minerals of different structural order, Clay Clay Miner. 59 (2011) 116–135.
[61] J. Du, G. Morris, R.A. Pushkarova, R.S. Smart, Effect of surface structure of kaolinite on aggregation, settling rate, and bed density, Langmuir 26 (2010) 13227–13235.
[62] Z. Li, L. Schulz, C. Ackley, N. Fenske, Adsorption of tetracycline on kaolinite with pH-dependent surface charges, J. Colloid Interface Sci. 351 (2010) 254–260.
[63] Y. Wu, Y. Si, D. Zhou, J. Gao, Adsorption of diethyl phthalate ester to clay minerals, Chemosphere 119 (2015) 690–696.
[64] M.R. Abukhadra, B.M. Bakry, A. Adlii, S.M. Yakout, M.E. El-Zaidy, Facile conversion of kaolinite into clay nanotubes (KNTs) of enhanced adsorption properties for toxic heavy metals (Zn^{2+}, Cd^{2+}, Pb^{2+}, and Cr^{6+}) from water, J. Hazard Mater. 374 (2019) 296–308.
[65] Q. Zhang, J. Wang, Y. Zhang, J. Chen, Natural kaolinite-based hierarchical porous microspheres as effective and highly recyclable adsorbent for removal of cationic dyes, Environ. Sci. Pollut. Res. Int. 29 (2022) 72001–72016.
[66] Y. Zhao, E. Abdullayev, A. Vasiliev, Y. Lvov, Halloysite nanotubule clay for efficient water purification, J. Colloid Interface Sci. 406 (2013) 121–129.
[67] M.H. Shamsi, K.E. Geckeler, The first biopolymer-wrapped non-carbon nanotubes, Nanotechnology 19 (2008) 1–5.
[68] T.H. Nguyen, K.L. Chen, Role of divalent cations in plasmid DNA adsorption to natural organic matter-coated silica surface, Environ. Sci. Technol. 41 (2007) 5370–5375.
[69] P. Cai, Q. Huang, W. Chen, D. Zhang, K. Wang, D. Jiang, W. Liang, Soil colloids-bound plasmid DNA: effect on transformation of E. coli and resistance to DNase I degradation, Soil Biol. Biochem. 39 (2007) 1007–1013.